PHYSICAL REVIEW B **81**, 155307 (2010)

Charge hopping revealed by jitter correlations in the photoluminescence spectra of single CdSe nanocrystals

Mark J. Fernée,* Brad Littleton,† Taras Plakhotnik, and Halina Rubinsztein-Dunlop
Centre for Quantum Computer Technology, School of Physical Sciences, The University of Queensland, Queensland 4072, Australia

Daniel E. Gómez‡ and Paul Mulvaney
School of Chemistry, The University of Melbourne, Parkville, Victoria 3010, Australia

(Received 2 February 2010; published 8 April 2010)

Spectral fluctuations observed in single CdSe/ZnS nanocrystals at 5 K are found to be entirely the result of discrete charge hops in the local environment of the nanocrystal, which occur at a rate comparable to the acquisition time of a single spectrum. We show that intervals between discrete spectral hops introduce a correlation between the successive measurements of the emission wavelength of single CdSe nanocrystals. This correlation can be recovered even in the presence of noise, but is shown to be sensitive to the experimental acquisition time, in good agreement with theory. However, we only find correlations for the smaller of the two nanocrystal sizes studied and discuss this in terms of size-dependent time scales correlated with the amount of excess energy dissipated in the nanocrystal due to hot-carrier relaxation.

DOI: 10.1103/PhysRevB.81.155307 PACS number(s): 78.67.Bf, 78.55.Et

I. INTRODUCTION

Electrical conductivity in polymers and other disordered soft condensed media is a complex problem that has seen much attention.[1] Charge transport in these materials is commonly described by charge-hopping models.[2–7] These models can cover a range of different charge transport mechanisms from quick hopping through a large density of shallow trap states (this can be viewed as quasicontinuous drift) to slower percolating transport through deep trap states[7] (also know as discrete-jump model). The distinction between hopping and continuous transport is time-scale dependent. If the charge motion is averaged over times much longer than the expected time between jumps, a large number of discrete jumps will result in apparently continuous drift. Thus, discrete hopping regime can be interpreted as the one where the probability of having no jumps during the averaging period is close to 1. The continuous regime corresponds to this probability being negligible (that is very close to zero). Although variable range hopping theoretical models have been applied with considerable success, direct detection of discrete charge-hopping assumed in these materials has so far not been attempted.

Semiconductor nanocrystals (NCs) present a physically interesting and practically useful prototypical system for studying charge transport. Excitonic transitions in NC quantum dots are extremely sensitive to electric field fluctuations in their local environment, which manifest as spectral diffusion (SD) (Refs. 8–11); a spectral line shift attributed to the linear Stark effect.[10] The linear Stark shift implies the presence of large internal electric fields in these materials[10] and makes NCs extremely sensitive to local charge motion. For example, based on polarizability measurements of single CdSe NCs,[9] 0.6 nm displacement (a lattice constant of CdSe is 5.81 Å) of a single charge located 5 nm from the core of a NC, will be readily detectable as a spectral shift of order of 100 μeV. The use of single NCs as probes of environmental charge has been demonstrated using engineered asymmetrical NCs consisting of a spherical CdSe core encapsulated in a CdS rod,[12,13] where the position of a single charge carrier introduces a correlation between the spectral peak position and the line width. However, the charge transport mechanism was not probed, but assumed to be diffusive;[12] due to a spatially uniform density of shallow electron traps at the surface.

Large "instantaneous" charge displacement in NCs has been suggested as a cause of steplike "off" events in the photoinduced emission.[14] This picture was supported by direct detection of ionization events in single CdSe NCs using electron force microscopy.[15] Furthermore, large spectral shifts were found following blinking off events, further supporting the charge displacement hypothesis.[14] Large discrete spectral jumps were also observed in the first spectroscopic studies of single nanocrystals, which also suggest large charge displacements occur during continuous emission. We recently confirmed this interpretation with the first spectroscopic evidence for jumping between different charge states, which requires trapping of one of the charge carriers.[16] These charge rearrangements phenomena are typically long lived and easily detected in spectroscopic time series. However statistical analyses of the spectral shifts observed in long time series of successive spectra obtained during continuous "on" periods reveal that large spectral jumps are relatively uncommon and that a small spectral jitter[13] dominates during continuous emission times with peak shifts on the order of a fraction of a milli-electron-volt observed at low temperatures. This jitter has been characterized with a Lorentzian distribution of jump amplitudes with the distribution width independent of temperature below 50 K, but dependant on the energy of the nonresonant pump.[11–13] This latter property links the spectral jitter to hot-carrier relaxation following excitation with a nonresonant pump.

The presence of SD during the integration time of the experiment broadens the measured spectral line width. Such broadening depends on the time scale of the spectral jitter relative to the time scale of the spectral measurement. Em-

pedocles and Bawendi[11] attributed this spectral jitter to a charge rearrangement among an ensemble of bimodal traps, although a time scale of the dynamics could not be determined from their data. Palinginis *et al.*[17,18] first probed the spectral line width using an ensemble hole burning technique and found a time scale of the order of a microsecond was required to overcome the spectral jitter in order to recover a line width of 6 μeV. A recent report using a sophisticated photon correlated Fourier spectroscopy on single CdSe NCs reported a line width of 6.5 μeV at a time scale of 100 μs, and an additional SD contribution of 4 μeV was also independently recovered.[19] Interestingly, the growth of the SD contribution to the line width was found to saturate at approximately 12 μeV at millisecond time scales.[19] This result is seemingly at odds with the analysis of Frantsuzov and Marcus[20] who fit the data of Empedocles and Bawendi[11] with a quasicontinuous charge diffusion model and find the linewidth saturates at $\sim$3 meV on the 100 s time scale. While the two experimental results present different energy scales and different time scales, the quasicontinuous diffusion analysis only admits saturation at one time scale, not both.

This question of a time scale for SD is also interesting from another perspective; the widely studied topic of photoluminescence blinking is known to be scaleless, obeying power-law statistics.[21] As blinking is believed to involve rapid charge rearrangement, which itself gives rise to SD, one may expect to find a similar distribution of SD time scales. Reports investigating this SD are compatible with both continuous charge motion[17–20] and a hopping mechanism.[11,22,23] Statistics of this jitter was the focus of our experiments.

In this paper we introduce a technique capable of distinguishing between the statistics of discrete and continuous charge motion detected as a Stark shift of a single emitter. We apply this technique to the analysis of spectral peak jitter of single CdSe/ZnS nanocrystals and find significant correlations in the time series of spectral jump magnitudes, which are extremely sensitive to both the NC size and experimental integration time (as predicted by the theory). The presence of significant correlation shows that spectral peak jitter is dominated by discrete charge hops, rather than diffusive continuous charge motion.

II. EXPERIMENT

Spectroscopic measurements were made on single CdSe/ZnS core/shell NCs of two different sizes (Invitrogen ITK605, ITK655 with core radii approximately 2.5 and 4 nm respectively[24]). Samples were prepared by diluting the stock solution with decane to a concentration of 10^{-11} M and spin coating on a crystal quartz substrate. The NCs were deposited directly on the quartz substrate without a supporting polymer matrix. The sample was loaded into a continuous flow liquid He cryostat (Oxford Microstat) and the sample chamber evacuated using a turbo pump. The cold finger could be cooled to temperatures approaching 3 K. A 0.5 W 532 nm diode pumped solid-state laser was used to provide wide field illumination of the sample using an epifluorescence geometry. The signal was collected by a long working distance objective (Nikon, NA 0.7 100×), filtered to remove the excitation line and passed to a 300 mm imaging spectrometer (Acton 300i) using a 2400 l/mm grating, giving a spectral resolution of 80 μeV. Spectra were recorded using an electron multiplying charge-coupled device (CCD) camera (Andor iXon) allowing relatively short exposures and high frame rates.

III. RESULTS

Approximately 10% of the NCs had narrow spectral lines close to the resolution limit, and these were selected for the study. The data were taken as long kinetic series of successive emission spectra at a sample temperature of 5 K. All NCs exhibited SD. A series of 512 successive spectra taken from a single $R\sim 2.5$ nm NC is shown in Fig. 1. A section with relatively little fluctuation is expanded to reveal a series of 40 individual spectra and a histogram of spectral peak positions is indicated below the kinetic series. Successive spectra can be aligned relative to the position of the spectral peak, and the efficacy of this process is illustrated by the ability to generate a narrow average spectrum [Fig. 1(d)].[25] Inspection of individual spectra [Fig. 1(b)] reveals that SD during the integration period is the dominant factor broadening the peak; however, it has far less influence on the line width than has previously been reported for single CdSe/ZnS NCs,[8–11] which may be attributable to improvements in NC synthesis.

Single CdSe NCs excited above their band edge must first relax to the $(1S_e1S_{3/2})$ exciton state before radiative carrier recombination occurs. This hot-carrier relaxation has been shown to drive SD through the generation of optical phonons that interact with the local charge environment.[11–13] Such a process is well described by Poissonian statistics.[20]

As SD is caused by random fluctuations of the NCs environment, there may be several microscopic sources of these fluctuations. Each of these sources can have several discrete states and the dynamics result from superposition of elementary jumps between these states. If these jumps are uncorrelated, the statistics of spectral jumps should be described by Poissonian statistics. The probability for detecting a spectral jump of magnitude, ν, is of the form,[26]

$$P_\Sigma(\nu) = \sum_{n=0}^{\infty} B_n(N) P_n(\nu), \tag{1}$$

comprising a weighted sum over the individual probability distributions, $P_n(\nu)$ for n jumps occurring, and the probability of no jump occurring is given by the Dirac delta function, $P_0(\nu)=\delta(\nu)$. The weight factors are determined by the Poisson distribution, $B_n(N)=N^n \exp(-N)/n!$ where N represents the average number of jumps per exposure. The individual probabilities, $P_n(\nu)$ can be provided by a microscopic model for SD.[26]

In Figs. 2(a) and 2(b) we plot the spectral jump histograms obtained from two single NCs with $R\sim 2.5$ nm and $R\sim 4$ nm cores, respectively. Both histograms are reasonably well fit with Lorentzian curves and are remarkably similar.

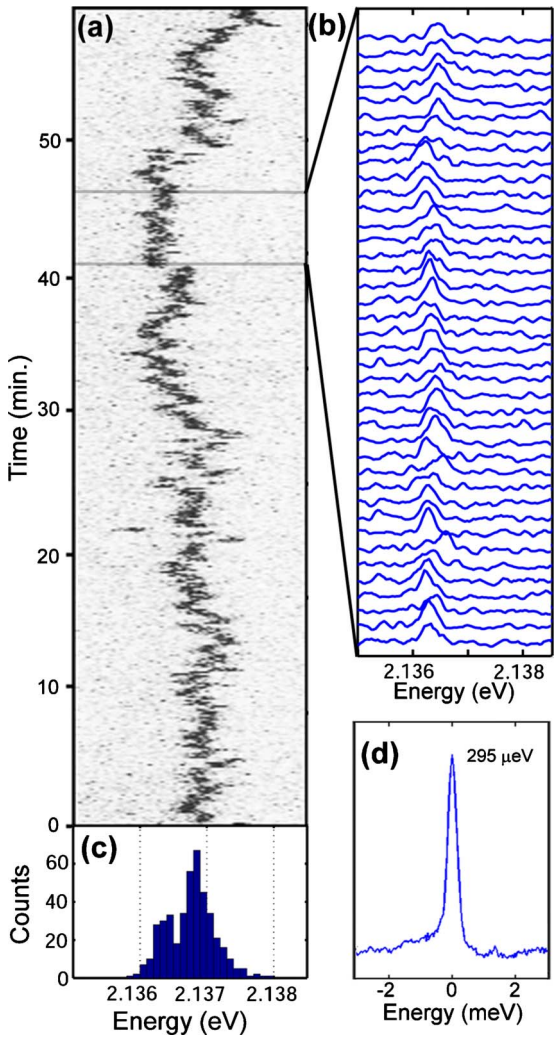

FIG. 1. (Color online) (a) A series of 512 successive spectra obtained from a single NC of $R\sim 2.5$ nm at 5 K using a pump irradiance of 27 W/cm^{-2} and a 7 s integration time. (b) An expanded region of greater stability illustrating the effect of SD on individual spectra. (c) A histogram of peak locations for the data in (a). (d) Average spectrum obtained by aligning each spectrum to its peak position (peak FWHM=295 μeV).

A striking difference is revealed when we plot $P(|\nu_n| \leq \Delta \,||\, \nu_{n-1}| \leq \Delta)$, the conditional probability of detecting two jumps smaller than Δ separated by $l-1$ jumps (for example, $l=1$ corresponds to two consecutive jumps).

Plots (c) and (d) use spectral jump time series that generated the data in (a) and (b), respectively, and we find a large correlation for the $R\sim 2.5$ nm core NC evident as an increase in probability around $l=1$ standing $\sim 7\sigma$ above the mean (i.e., $P(|\nu_n| \leq \Delta \,||\, \nu_{n-1}| \leq \Delta) - \bar{P} = 0.098$, $\sigma_P = 0.015$). No such correlation exists for the $R\sim 4$ nm core NC (i.e., $P(|\nu_n| \leq \Delta \,||\, \nu_{n-1}| \leq \Delta) - \bar{P} = 0.012$, $\sigma_P = 0.015$). In (e) and (f) we plot the conditional probability using spectral jump time series obtained by concatenating approximately 20 shorter time series obtained from individual NCs of the same 2.5 nm and 4 nm core radius, respectively [not including the data of (c) and (d)]. Again we see a strong correlation in the data from the smaller $R\sim 2.5$ nm NCs and no correlation in the data from the $R\sim 4$ nm NCs, which suggests that the correlations are characteristic of the smaller $R\sim 2.5$ nm NCs.

Theoretically, $P(|\nu| \leq \Delta) = B_0^2$ in the limit of $\Delta = 0$ because $|\nu| = 0$ is possible only if no jumps happened during *two consecutive* measurements. The probability of two consecutive jumps of zero amplitude is B_0^3 [as illustrated in Fig. 3(a)]. Therefore the conditional probability $P(|\nu_n| = 0 \,||\, \nu_{n-1}| = 0) = B_0$. For not consecutive jumps $P(|\nu_n| = 0 \,||\, \nu_{n-l}| = 0) = B_0^2$ [as illustrated in Fig. 3(b)].

We plot the correlation, $C \equiv P(|\nu_n| = 0 \,||\, \nu_{n-1}| = 0) - P(|\nu_n| = 0) = B_0(1 - B_0)$ in Fig. 4 and find that it is strongly peaked around $N = 0.7$, and therefore the presence of such correlations will provide a statistical indication of a low jump rate in otherwise random jump data. However, measurement error caused by the Poissonian statistics of the photo counts, background noise combined with frequency shifts caused by SD observed at shorter time scales,[17–19] introduce additional fluctuations of the transition frequency, making the jump analysis more complicated. The influence of these additional fluctuations can be eliminated by setting the value of Δ significantly larger than the fluctuations. The peak measurement error depends sensitively on the signal-to-noise ratio of each spectrum. We determined the peak measurement error by measuring a series of spectra obtained from a 632 nm HeNe laser spot attenuated to lie in signal-to-noise range of the single NC measurements (which approximates a delta function at the resolution of our instrument) and find a standard deviation, $\sigma_M \sim 20$ μeV. In the data analysis the value of Δ was set at 60 μeV, which maximized the correlation, thus accounting for *all* additional fluctuations. The effect of the bin width, Δ on the strength of the correlation is shown in Fig. 5 where we plot the correlation, $C \equiv P(|\nu_n| \leq \Delta \,||\, \nu_{n-1}| \leq \Delta) - P(|\nu_n| \leq \Delta)$ as a function of bin width. If we set Δ too small we see a dip in C due to the combined effect of measurement error as well as any additional fluctuations at faster time scales. For large Δ the correlation also decreases. These features are perfectly captured in a simulated SD data set comprising 10^5 data points. Here the model simply considers a Lorentzian distribution of random jumps [full width at half maximum (FWHM)=200 μeV similar to the distribution in Fig. 2(a)] occurring at a rate, N, along with a Gaussian distributed measurement error. All three parameters are determined independently from experimental data and *no* adjustable parameters were used to obtain the fit. The time series of peak positions is then determined according to (using the notation in Fig. 3), $p_n = p_{n-1} + \Sigma_i \nu_i \Delta t_i / T + \varepsilon_i$, where the second term is the average jump frequency during the integration time, T, obtained by summing over all the spectral jumps that occur during the integration period, ν_i weighted by the time between jumps, Δt_i. The last term is a Gaussian distributed random variable with $\sigma = 20$ μeV (equal to our peak measurement error, σ_M). The model used to generate the simulated data clearly captures the behavior of the experimental data, indicating that peak measurement error, σ_M alone is sufficient to account for the dip at low Δ. This limits the magnitude of any fluctuations caused by SD at faster time scales[17–19] to below the 20 μeV peak measurement resolution of our experiment. In general the simulation model demonstrates the general principle that correlations can be found in time series of purely random frequency jumps using

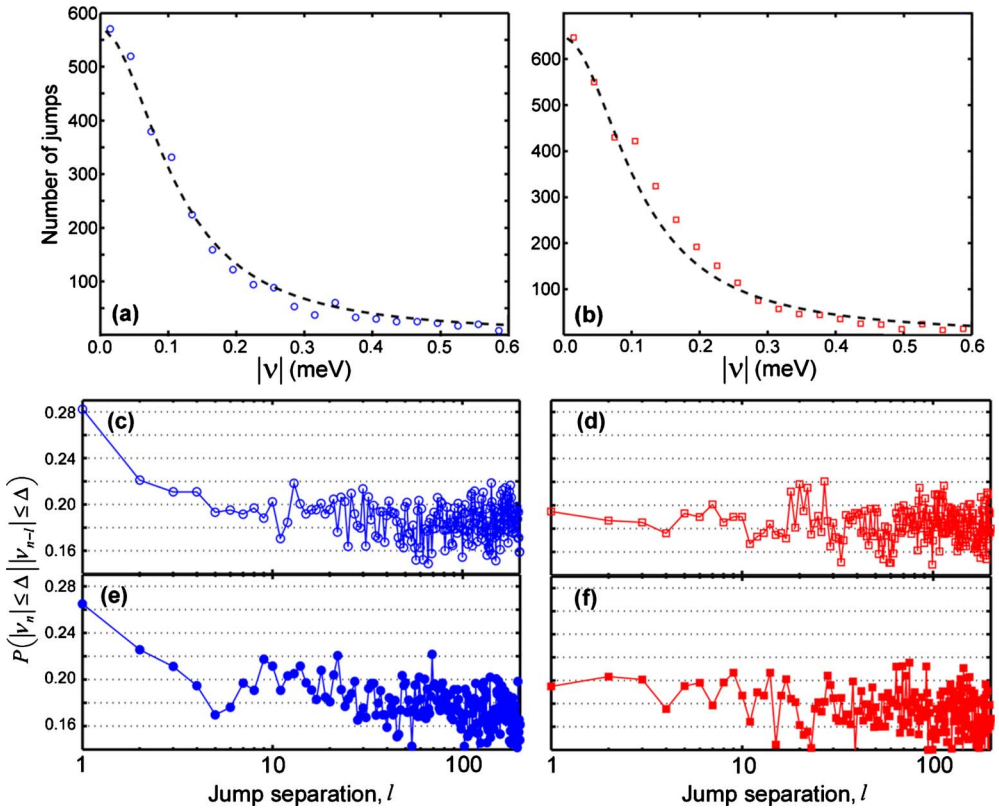

FIG. 2. (Color online) (a) Histogram of spectral jump magnitudes (blue circles—bin width 30 μeV) obtained from a series of 3163 individual 1 s spectra from a single $R \sim 2.5$ nm core diameter NC with a pump irradiance of 66 W/cm^2. (b) Histogram of spectral jump magnitudes (red squares—bin width 30 μeV) obtained from a series of 3552 individual 1 s spectra from a single $R \sim 4$ nm core diameter NC with a pump irradiance of 52 W/cm^2. The dashed lines represent Lorentzian fits to the data. Panels (c)–(f) show conditional probability $P(|\nu_n| \le \Delta \,||\nu_{n-l}| \le \Delta)$ as a function of the jump separation, l, with $\Delta = 60$ μeV. (c) Single $R \sim 2.5$ nm core diameter NC shown in (a) (blue open circles). (d) Single $R \sim 4$ nm core diameter NC shown in (b) (red open squares). (e) Ensemble of 20 single $R \sim 2.5$ nm NCs comprising 2945 jumps. (f) Ensemble of 21 single $R \sim 4$ nm NCs comprising 2339 jumps. 60 μeV bin widths are used throughout.

the analysis of frequency differences as outlined in Fig. 3 for sufficiently low jump rates, as indicated by Fig. 4. The only requirement is that the jump rate, N, be well defined, which implies a well-defined time scale for SD.

With $\Delta \neq 0$ the probability must include additional terms, $P(|\nu| \le \Delta) = B_0^2 + P_D + 2B_0 P_\Delta$, where P_D is the probability of getting $|\nu| \le \Delta$ as a result of codirectional dynamics in the system (the frequency jumps in the same direction during the two integration times and the magnitudes of the jumps are close) and P_Δ is the probability of getting a jump smaller than Δ in one of the measurements. The probability of two consecutive jumps of $|\nu| \le \Delta$ amplitudes is then $B_0^3 + 3B_0^2 P_\Delta + B_0 P_\Delta^2 + P_D^2$. Here we have added probabilities of three consecutive integration intervals with the following characteristics: three "no jump" intervals, three possibilities of two "no jump" intervals and one Δ jump, two Δ-jump intervals separated by one "no jump" interval, and two pairs of intervals with codirectional dynamics. The probabilities B_0, P_D, and P_Δ are assumed to be uncorrelated. Next we suppose for simplicity (see below) that $P_\Delta \approx P_D$. This is a reasonable assumption if the distribution function of the frequencies has a broad (relatively to Δ) flat top around zero. Thus, we derive the following approximate relations:

$$P(|\nu| \le \Delta) \approx B_0^2 + 2B_0 P_D + P_D, \tag{2}$$

$$P(|\nu_n| \le \Delta \,||\nu_{n-1}| \le \Delta) \approx \frac{B_0^3 + 3B_0^2 P_D + (B_0 + 1)P_D^2}{B_0^2 + 2B_0 P_D + P_D}. \tag{3}$$

Note that if $B_0 = 0$, then $P(|\nu_n| \le \Delta \,||\nu_{n-1}| \le \Delta) = P(|\nu| \le \Delta)$. Spikes in Figs. 2(c) and 2(e) suggest that $B_0 \neq 0$.

We have tested Eqs. (2) and (3) using simulated SD data comprising 10^5 data points (and including a $\sigma_M = 25$ μeV peak measurement error) with well-defined jump rates, N and find the correlation spike to be sensitive to the jump rate as predicted. However, due to the approximation $P_\Delta \approx P_D$ made in deriving Eqs. (2) and (3), we find that they are only able to predict the value of N to within 20% (although this level of accuracy is more than sufficient to categorize the overall jump rate). The sensitivity of Eqs. (2) and (3) to the choice of the parameter, P_Δ can be simply demonstrated by setting P_Δ anywhere in the interval $0 \le P_\Delta \le 0.5$, where we find the solution for B_0 satisfies the inequality $0.12 < B_0 < 0.37$ corresponding to $2.1 \ge N \ge 1$. Therefore Eqs. (2) and (3) still provide a good estimation of the jump rate, N, without requiring more detailed knowledge of the distribution function and the underlying process'.

From the experimental data shown in Fig. 2(c) one can determine that $P(|\nu| \le \Delta) \approx 0.2$ and $P(|\nu_n| \le \Delta \,||\nu_{n-1}| \le \Delta) \approx 0.28$. Equations (2) and (3) can be then used to find that

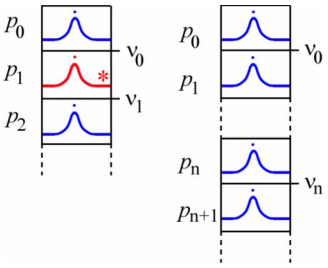

FIG. 3. (Color online) Spectral jump time series are generated from calculating the difference between two successive spectral peak measurements, $\nu_n = p_{n+1} - p_n$. Correlations between successive spectral jumps in spectral jump time series can arise from the presence of a common spectrum (asterisk) in the case when calculating the joint probability for observing two intervals with no jumps (i.e., $|\nu| = 0$). Only three spectra are required when calculating the joint probability for successive jumps to have zero magnitude (a), while four spectra are required in all other cases (b).

$P_D \approx 0.06$ and $B_0 \approx 0.32$. Such a value of B_0 corresponds to 1 jump per integration time on average.

Doubling the integration time makes $B_0 = 0.32^2 \approx 0.1$ and from Eq. (2) and $P(|\nu| \leq \Delta) \approx 0.2$ it follows that $P_D \approx P_\Delta \approx 0.17$. For these values of B_0, P_D, and P_Δ, Eq. (3) predicts that the conditional probability $P(|\nu_n| \leq \Delta \,||\, \nu_{n-1}| \leq \Delta) \approx 0.19$.

We have tested this prediction by adding pairs of successive spectra from the data used in Figs. 2(a) and 2(d), thus effectively doubling the integration time. The results are shown in Fig. 6 where we find the value of $P(|\nu_n| \leq \Delta \,||\, \nu_{n-1}| \leq \Delta) \approx 0.18$ for the increased integration time.

IV. DISCUSSION

We see in Figs. 2(d) and 2(f) that data from the larger $R \sim 4$ nm core size NCs show no correlation visible above the noise. While this seems odd, we attribute the lack of observable correlation in the larger NCs to increased hot-carrier relaxation as discussed below. While all data sets comprise a range of CCD integration times and pump irradiances, the individual spectra all shared a comparable signal-to-noise ratio (SNR), indicating the rate of photon detection to be approximately constant over all the NCs studied. Given, the emission from a CdSe NC has been found to result from a degenerate dipole plane, there is no dim/dark axis and only

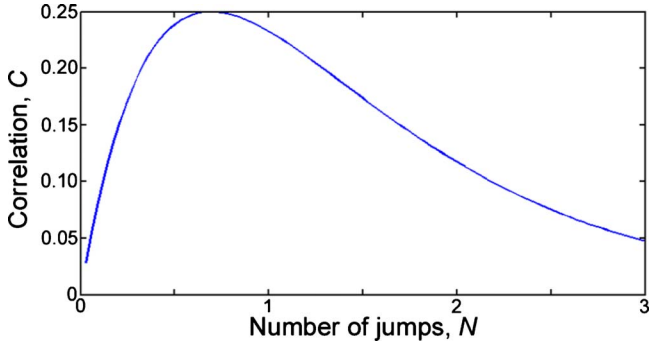

FIG. 4. (Color online) Variation in the correlation, C, as a function of the average number of spectral jumps, N.

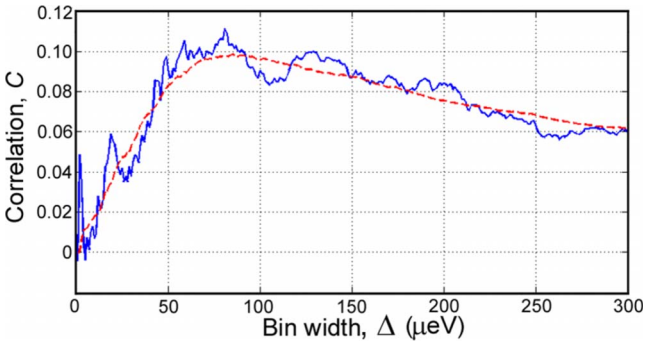

FIG. 5. (Color online) Variation in the correlation, C as a function of the bin width, Δ for the data of Fig. 2(c) (blue solid line). The same analysis applied to a 10^5 point simulated SD data set generated using Lorentzian distribution of random jumps with a FWHM of 200 μeV with an average jump rate $N = 1$ and a Gaussian peak measurement error with $\sigma_M = 20$ μeV (red dashed).

the photon polarization varies as a function of NC crystal orientation relative to the detection axis.[27] Thus, for a system with unity quantum yield,[28] the SNR provides a relative measure of the photon absorption rate, which is approximately constant in our measurements. Now, the $R \sim 2.5$ nm core NC has a band edge near 2.12 eV and we are pumping with 2.33 eV photons, generating hot charge carriers with 210 meV of excess energy that is dissipated primarily as optical phonons. The larger $R \sim 4$ nm core NC has a band edge near 1.97 eV, leaving 360 meV to be dissipated. It has long been established that hot-carrier relaxation drives SD at low temperatures with the jump distribution scaling linearly with photon energy (and hence excess carrier energy).[11,13] If we assume

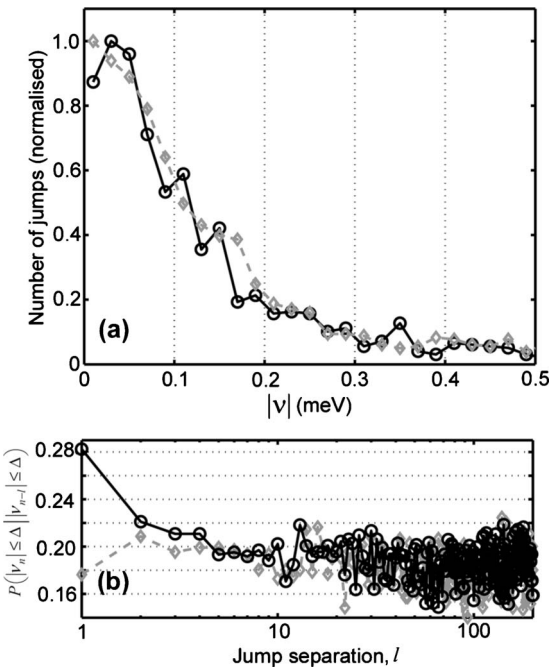

FIG. 6. (a) Jump distributions for the data in Fig. 2(a) with 15 μeV bin widths, using 1 s (open circles) and 2 s (open diamonds) integration times. (b) Conditional probabilities $P(|\nu_n| \leq \Delta \,||\, \nu_{n-l}| \leq \Delta)$, $\Delta = 60$ μeV.

that the optical phonons drive the fluctuating environmental charge with a constant coupling efficiency, the average number of jumps, N, will scale linearly with the amount of excess energy, from which we predict, $P(|\nu_n| \leq \Delta \,||\, \nu_{n-1}| \leq \Delta) \approx 0.19$ in close agreement with Fig. 2(d). However, given the relatively poor accuracy of Eqs. (2) and (3) discussed above, there is insufficient predictive power to make a strong claim, based on hot-carrier relaxation alone. Additionally, deviations from linear coupling as well as increases in surface area may also contribute to size sensitivity. For example; as SD is compatible with a surface-related phenomenon, we may also expect a concomitant increase in the jump rate with increasing surface area, which will further increase the sensitivity of the jump rate to nanocrystal size. In any case, the observed size dependence of the correlation serves as a convenient test of the analysis that also excludes any trivial origin of the correlation, as well as illustrating the sensitivity of the correlation to nontrivial materials factors.

While we here have not observed correlations from the larger $R \sim 4$ nm NCs, a comparatively low spectral jump rate is implied by our previous observation that line widths below 20 μeV can still be observed out to even longer integration times in these NCs using very low SNRs.[23] Given the jump histograms shown in Fig. 2 are characteristic of the most stable NCs we have observed, a measurement of any line width appreciably narrower than these histograms indicates that the spectral jump rate must be extremely low in order to inhibit inhomogeneous broadening.

The time scale for the process causing the observed SD is more appropriately expressed as a jump probability per absorbed photon (assuming unit quantum efficiency at 5 K) and is $\sim 10^{-4}$ jumps/absorbed photon for $N \sim 1$, indicating that the process driving the observed spectral diffusion is only weakly coupled to the excitation of the nanocrystal. Time scales for SD have been discussed in a number of previous reports in the context of high resolution linewidth measurements.[17–20,22] These studies report considerably shorter time scales are required to overcome SD. However, in the recent report of Coolen *et al.*[19] studying single CdSe/ZnS NCs at cryogenic temperatures, the SD contribution was found to saturate at a value of ~ 12 μeV, on a millisecond time scale, which is below the resolution of our experiment and thus compatible with our result. Taken together, these results indicate the that SD we observe must originate from a physical process distinct from to that which causes SD over millisecond time scales and that this longer time-scale process dominates the SD that is commonly observed in low temperature single NC spectroscopy. Furthermore, our paper provides a statistical approach that can distinguish between two SD processes occurring at different time scales and shows that *all* SD detected within the resolution of our experiment are comprised of discrete events.

Finally we point out that our paper is primarily concerned with establishing a time scale for SD. We have established that the spectral shifts occur as discrete jumps rather than a continuous drift. However, it is still not yet been shown that the cause of the SD is charge motion around the NC, although the phenomenon is entirely consistent with this and so we adopt this interpretation in this paper. Nevertheless, our technique provides a statistical technique capable of distinguishing between the different types of charge motion.

V. CONCLUSION

We have introduced a statistical method that can distinguish between continuous and discrete evolution of a measured time series by correlating successive periods between discrete jumps. This method was applied to the analysis of jitter in the emission spectral peak obtained from single CdSe/ZnS NCs, revealing the *entirety* of the measurable jitter to be caused by discrete charge hops in the NCs local environment that occur at a rate comparable to the time scale of the experiment. This is consistent with charge hops between deep potential wells, rather than diffusive charge motion through a manifold of shallow potentials and reveals that SD is only weakly coupled to the optical pump. Moreover, our result discriminates between two distinct time scales in SD and shows that the SD phenomenon does not follow that scaleless behavior found in photoluminescence blinking.

In general, this result demonstrates the use of single NCs as sensitive spectroscopic probes of charge motion in their local environment. With resonant or near resonant excitation, the intrinsic photoinduced SD can be avoided[29] so that single NCs may be used to test charge transport mechanisms in different media surrounding the NCs.

ACKNOWLEDGMENT

This work was supported by the Australian Research Council.

*FAX: +61 7 3365 1242; fernee@physics.uq.edu.au

†Present address: Dept. of Physics, King's College London, the Strand, London WC2R 2LS, United Kingdom.

‡Present address: Materials Science and Engineering, CSIRO, Private Bag 33, Clayton South MDC, Victoria 3169, Australia.

[1] *Charge Transport in Disordered Solids with Applications in Electronics*, edited by S. Baranovski (Wiley, West Sussex, 2006).

[2] V. Coropceanu, J. Cornil, D. A. Da Silva Filho, Y. Olivier, R. Silbey, and J. L. Bredas, Chem. Rev. **107**, 926 (2007).

[3] F. C. Grozema and L. D. A. Siebbeles, Int. Rev. Phys. Chem. **27**, 87 (2008).

[4] D. L. Cheung, D. P. McMahon, and A. Troisi, J. Am. Chem. Soc. **131**, 11179 (2009).

[5] H. Sirringhaus, P. J. Brown, R. H. Friend, M. M. Neilsen, K. Bechgaard, B. Langeveld-Voss, A. Spiering, R. Janssen, E. W. Meijer, P. Herwig, and D. M. De Leeuw, Nature (London) **401**, 685 (1999).

[6] S. L. M. van Mensfoort, J. Billen, S. I. E. Vulto, R. A. J. Janssen, and R. Coehoorn, Phys. Rev. B **80**, 033202 (2009).

[7] U. Wolf, H. Bassler, P. M. Borsenberger, and W. T. Gruenbaum, Chem. Phys. **222**, 259 (1997).
[8] S. A. Empedocles, D. J. Norris, and M. G. Bawendi, Phys. Rev. Lett. **77**, 3873 (1996).
[9] S. A. Empedocles and M. G. Bawendi, Science **278**, 2114 (1997).
[10] S. A. Empedocles, R. Neuhauser, K. Shimizu, and M. G. Bawendi, Adv. Mater. **11**, 1243 (1999).
[11] S. A. Empedocles and M. G. Bawendi, J. Phys. Chem. B **103**, 1826 (1999).
[12] J. Muller, J. M. Lupton, A. L. Rogach, J. Feldmann, D. V. Talapin, and H. Weller, Phys. Rev. Lett. **93**, 167402 (2004).
[13] J. Muller, J. M. Lupton, A. L. Rogach, J. Feldmann, D. V. Talapin, and H. Weller, Phys. Rev. B **72**, 205339 (2005).
[14] R. G. Neuhauser, K. T. Shimizu, W. K. Woo, S. A. Empedocles, and M. G. Bawendi, Phys. Rev. Lett. **85**, 3301 (2000).
[15] T. D. Krauss and L. E. Brus, Phys. Rev. Lett. **83**, 4840 (1999).
[16] M. J. Fernée, B. N. Littleton, and H. Rubinsztein-Dunlop, ACS Nano **3**, 3762 (2009).
[17] P. Palinginis and H. Wang, Appl. Phys. Lett. **78**, 1541 (2001).
[18] P. Palinginis, S. Tavenner, M. Lonergan, and H. Wang, Phys. Rev. B **67**, 201307(R) (2003).
[19] L. Coolen, X. Brokmann, P. Spinicelli, and J.-P. Hermier, Phys. Rev. Lett. **100**, 027403 (2008).
[20] P. A. Frantsuzov and R. A. Marcus, Phys. Rev. B **72**, 155321 (2005).
[21] P. A. Frantsuzov, M. Kuno, B. Janko, and R. A. Marcus, Nat. Phys. **4**, 519 (2008).
[22] L. Coolen, P. Spinicelli, and J.-P. Hermier, J. Opt. Soc. Am. B **26**, 1463 (2009).
[23] B. N. Littleton, M. J. Fernée, D. E. Gomez, P. Mulvaney, and H. Rubinsztein-Dunlop, J. Phys. Chem. C **113**, 5345 (2009).
[24] T. J. Liptay, L. F. Marshall, P. S. Rao, R. J. Ram, and M. G. Bawendi, Phys. Rev. B **76**, 155314 (2007).
[25] M. J. Fernée, B. N. Littleton, S. Cooper, H. Rubinsztein-Dunlop, D. E. Gómez, and P. Mulvaney, J. Phys. Chem. C **112**, 1878 (2008).
[26] T. Plakhotnik, E. A. Donley, and B. M. Kharlamov, Phys. Rev. Lett. **87**, 015504 (2001).
[27] S. A. Empedocles, R. Neuhauser, and M. G. Bawendi, Nature (London) **399**, 126 (1999).
[28] Y. Ebenstein, T. Mokari, and U. Banin, Appl. Phys. Lett. **80**, 4033 (2002).
[29] L. Biadala, Y. Louyer, Ph. Tamarat, and B. Lounis, Phys. Rev. Lett. **103**, 037404 (2009).